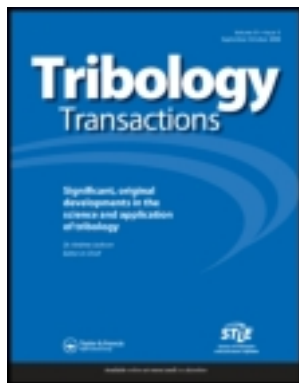


This article was downloaded by: [University of California Santa Barbara]

On: 01 March 2013, At: 10:50

Publisher: Taylor & Francis

Informa Ltd Registered in England and Wales Registered Number: 1072954 Registered office: Mortimer House, 37-41 Mortimer Street, London W1T 3JH, UK



## Tribology Transactions

Publication details, including instructions for authors and subscription information:

<http://www.tandfonline.com/loi/utrb20>

### Oxidation Chemistry of a Pentaerythritol Tetraester Oil

T. E. Karis<sup>a</sup>, J. L. Miller<sup>a</sup>, H. E. Hunziker<sup>a</sup>, M. S. de Vries<sup>b</sup>, D. A. Hopper<sup>c</sup> & H. S. Nagaraj<sup>d</sup>

<sup>a</sup> IBM Research Division, Almaden Research Center, San Jose, California, 95120

<sup>b</sup> The Hebrew University of Jerusalem, Department of Chemistry, Jerusalem, Israel, 91904

<sup>c</sup> Piedmont Hills High School, San Jose, California, 95132

<sup>d</sup> IBM Storage Systems Division, San Jose, California, 95193

Version of record first published: 25 Mar 2008.

To cite this article: T. E. Karis, J. L. Miller, H. E. Hunziker, M. S. de Vries, D. A. Hopper & H. S. Nagaraj (1999): Oxidation Chemistry of a Pentaerythritol Tetraester Oil, Tribology Transactions, 42:3, 431-442

To link to this article: <http://dx.doi.org/10.1080/10402009908982239>

PLEASE SCROLL DOWN FOR ARTICLE

Full terms and conditions of use: <http://www.tandfonline.com/page/terms-and-conditions>

This article may be used for research, teaching, and private study purposes. Any substantial or systematic reproduction, redistribution, reselling, loan, sub-licensing, systematic supply, or distribution in any form to anyone is expressly forbidden.

The publisher does not give any warranty express or implied or make any representation that the contents will be complete or accurate or up to date. The accuracy of any instructions, formulae, and drug doses should be independently verified with primary sources. The publisher shall not be liable for any loss, actions, claims, proceedings, demand, or costs or damages whatsoever or howsoever caused arising directly or indirectly in connection with or arising out of the use of this material.



# Oxidation Chemistry of a Pentaerythritol Tetraester Oil<sup>®</sup>

T. E. KARIS, J. L. MILLER and H. E. HUNZIKER

IBM Research Division  
Almaden Research Center  
San Jose, California 95120

M. S. de VRIES

The Hebrew University of Jerusalem  
Department of Chemistry  
Jerusalem, Israel 91904

D. A. HOPPER

Piedmont Hills High School  
San Jose, California 95132

and

H.S. NAGARAJ

IBM Storage Systems Division  
San Jose, California 95193

*Synthetic oils have come into widespread use due to their inherent stability, consistent physical properties, and reproducible composition. As ever increasing demands are being placed on oil performance in magnetic recording disk drives by increasing rotation rates up to 10,000 rpm, it is important to know the ultimate limitations of these functional fluids due to oxidation; In this study, the authors focus on a pentaerythritol ester oil. Accelerated aging tests were carried out on the oil at elevated temperature. Tests were also done with 50 ppm of dissolved iron in the oil. The progress of oxidation was followed by analytical techniques including UV/visible, infrared, and proton nuclear magnetic resonance spectroscopy, and gel permeation chromatography, thin layer chromatography, viscometry, and differential scanning calorimetry. A new technique of laser desorption mass spectrometry with jet cooling, which provides the parent ion mass spectrum, provided the mass distribution of intermediate oxidation products. These techniques enabled determination of the predominant oxidation products. Oxidation proceeds through interchain and intrachain proton abstraction. Hydroxyl groups form on alkyl chains. Intrachain proton abstraction leads to formation of oxetane and conjugated ketone on the original alkyl chain and to cleavage of the alkyl chain with the formation of methyl ketone and carboxylic acid end groups. Dissolved iron increased the formation rate of hydroxyl and oxetane without changing the hydroperoxide con-*

*centration. Oligomers were absent from the mass spectrum of the oxidized oil. The increase in oil viscosity with accelerated aging is due to increasing intermolecular hydrogen bonding between hydroxyl groups formed on alkyl chains.*

## KEY WORDS

Oxidation; Lubricants; Spectroscopy

## INTRODUCTION

Oxidation is one of the main factors limiting the useful lifetime of lubricating oils. As lubricants are being stressed to the limits of their performance capabilities in the aerospace, automotive, and disk drive industries, renewed efforts to understand the details of their oxidation chemistry are being undertaken. Extensive research on the class of synthetic lubricating oils made of organic esters has been previously carried out. One group studied the oxidation of tridecyl pelargonate, di-2-ethylhexyl sebacate, and trimethylol propane triheptanoate using the Penn State micro-oxidation test (1)-(5). Gel permeation chromatography was employed to measure the molecular weight of oxidation products. Increase in ultraviolet (UV) absorption upon oxidation was attributed to conjugated carbonyl and conjugated double bonds. From nuclear magnetic resonance spectroscopy (NMR), they identified the formation of ketones and a decrease in methylene protons. The oxidation was catalyzed by steel and copper.

A stirred flow micro-reactor was developed and used to study oxidation of n-hexadecane (6), (7). The oxidation products were identified by chemical analysis. A reaction scheme incorporating both interchain and intrachain proton abstraction was proposed to

interpret the results. Subsequent investigation by the same group employed the stirred flow micro-reactor to study oxidation of pentaerythritol tetraheptanoate (8). Their reaction mechanism accounts for the formation of hydroxyl groups, and the formation of carboxylic acid and methyl ketone end groups and chain cleavage through intrachain proton abstraction.

Thin film aging studies were done on pentaerythritol tetraheptanoate in aluminum pans (9). Gel permeation chromatography was employed to measure the molecular weight of oxidation products. Chemical analysis was done to identify oligomeric structures, and a reaction scheme was proposed.

The goal of this study was to characterize the oxidation chemistry during accelerated aging of a pentaerythritol tetraester lubricant base stock as the groundwork for development of additives to inhibit oxidation and metal ion catalysis. The relation between oxidation and changes in oil physical properties during oxidation was investigated. The authors identify the reactions producing the observed changes in UV absorbance, product mass spectrum, proton NMR peaks, glass transition temperature, thin layer chromatography, and viscosity. A vacuum UV laser desorption mass spectrometer with jet cooling and vacuum UV ionization was employed to measure the parent ion mass distribution of intermediate oxidation products. The role of dissolved iron in catalysis of the oxidation is considered.

## MATERIALS AND APPARATUS

The oil was a commercial pentaerythritol ester lubricant base stock. Dissolved iron was incorporated in the oil for some of the tests using iron (III) 2-ethylhexanoate, 52 percent in mineral spirits.

The UV absorbance spectra were measured with a diode array spectrophotometer. For the UV measurements, a drop of the oil was placed between two quartz disks (quartz wafer 25 mm diameter, 0.5 mm thick) and held in the beam during the wavelength scan. The absorbance reference was the pure oil prior to any aging.

NMR measurements were done in a Nuclear Magnetic Resonance Spectrometer with a 250 MHz super-conducting magnet. The solvent was chloroform- $d_1$  (99.8 atom % D,  $CDCl_3$ ). The samples were held in 5 mm NMR tubes. For the proton acquisitions, the spectrometer was set to a spectral width of 5000 Hz, a 45° pulse width of 3  $\mu$ sec, 2048 scans, and a relaxation delay of 1 sec.

Parent ion molecular mass spectra were obtained using a new type of mass spectrometer developed in the authors laboratory. The apparatus employs vacuum UV (125 nm, 10 eV) photoionization mass spectrometry with jet cooling to avoid fragmentation of the organic molecules. The apparatus is fully described in Ref. (10). The mass spectrometry technique is referred to here as laser desorption mass spectrometry (LDMS). Approximately 1-5 mg of the oil was deposited onto a pyrolytic graphite plate for the LDMS measurement. The LDMS spectra provide the only existing means to directly observe the mass distribution in a mixture of intermediate molecular weight organic compounds.

Viscosity measurements were done with a stress rheometer. A 2 cm diameter 1° cone was employed to minimize the sample size ( $\approx$ 200 mg).

The glass transition temperature of the aged oil was measured using a modulated differential scanning calorimeter.

Fourier Transform Infrared (FTIR) spectroscopy measurements were taken using NaCl plates (25x2 mm). Two NaCl plates were placed together and scanned as a background. A drop of oil was then placed between the two NaCl plates for the measurement. The spectrometer was set to scan from 500 to 4500  $1/cm$ . The background and sample were each scanned 64 times in a chamber that had been purged with nitrogen.

Gel permeation chromatograms (GPC) were measured using a column length of 300 mm, with styrene/divinylbenzene copolymer media, pore size 10 microns, and the solvent was tetrahydrofuran (THF). Four columns were used in series with a flow rate of 1 ml/min at 40°C. Calibration was done using 24 monodisperse polystyrene standards with different molecular weights between 500 and 3,000,000 Daltons.

Thin layer chromatography (TLC) measurements were done on the oil at various stages of accelerated aging. TLC measures the mobility of the oil in a solvent flow migrating along the surface of a 1x3 inch glass plate coated with 250  $\mu$ m of silica gel (60 Angstrom). The oil was deposited in a spot near one short edge of the plate as  $\approx$ 5 microliters of 5 wt.% oil solution in ethyl acetate. The ethyl acetate was allowed to dry, and the TLC plate was exposed in a TLC chamber for about one hour in mixed solvent n-heptane/ethyl ether 6/1 v/v as in Ref. (11). After exposure, the plate was removed from the TLC chamber, allowed to dry, and developed with iodine vapor in a sealed container at room temperature to observe how far the oil fractions had migrated along the silica gel. The migration rate of oil relative to the solvent front is decreased by increasing polarity, because the more polar species have a higher affinity for the silica gel.

Accelerated aging tests of the oil were done in an oven or in silicon oil baths at temperatures of 130°, 140°, 150°, 160° or 170°C, in air.

## PROCEDURE

The accelerated aging tests were done with five grams of oil in a 150 ml Pyrex beaker. This provided an oil film thickness of five mm. The beaker was covered by aluminum foil with a seven mm diameter hole near the center. Samples were taken each 24 hrs for analysis by drawing several drops of oil into a disposable glass pipette through the hole in the aluminum foil.

## RESULTS

Typical LDMS results are shown in Figs. 1 and 2. Molecular weights from the LDMS were truncated to their integer value. The mass values at which peaks were observed and the relative abundances are listed in Table 1. The abundance readings from the LDMS were scaled by shifting the baseline to zero and dividing by the abundance of the pentaerythritol tetrapentanoate (mass 472 in Table 1). The mass abundance for pure oil after aging 24 hrs at 150°C is shown in Fig. 1(a). Initial spectra were taken after 24 hrs at 150°C to eliminate volatile impurities that were present in the as-received oil. The molecular weight of the oil components are 472 for pentaerythritol tetrapentanoate (exact molecular weight 472.62), 528 for pentaerythritol tetrahexanoate (exact molecular

TABLE 1—MASS ABUNDANCE FOR THE PENTAERYTHRITOL TETRAESTER OIL IN VARIOUS STAGES OF OXIDATION AT 150°C. RELATIVE ABUNDANCE IS THE HEIGHT OF A MASS PEAK DIVIDED BY THE HEIGHT OF THE MASS PEAK AT 472. THE SOURCE OF THE MASS PEAKS (1) THROUGH (10) IS DESCRIBED IN THE TEXT. SOURCE TRANS. MAY BE DUE TO TRANSESTERIFICATION OF ALKYL ESTER CHAINS. MASS PEAKS FOR WHICH THE SOURCE WAS NOT IDENTIFIED ARE INDICATED BY --.

MASS	SOURCE	RELATIVE ABUNDANCE				
		24 HOURS		120 HOURS		264 HOURS
		PURE OIL	PURE OIL	OIL + 50 ppm IRON	PURE OIL	
402	--	0.00	0.04	0.01	0.15	
414	--	0.00	0.11	0.08	0.15	
416	7, 8	0.00	0.06	0.01	0.15	
428	--	0.05	0.15	0.13	0.21	
430	7	0.03	0.07	0.03	0.18	
444	7, 8	0.02	0.21	0.2	0.37	
458	7	0.01	0.08	0.09	0.27	
472	Original Oil	1.00	1	1	1	
486	2, 7, trans.	0.02	0.11	0.19	0.25	
488	3	0.02	0.08	0.06	0.19	
500	2, 7, 8, trans.	0.04	0.13	0.16	0.23	
504	3, 5,	0.01	0.02	0.07	0.04	
514	2, 7, trans.	0.06	0.13	0.13	0.24	
516	9	0.02	0.05	0	0.1	
528	Original Oil	1.26	1.11	1.01	0.91	
542	2, 7, trans.	0.04	0.18	0.29	0.38	
544	3	0.01	0.1	0.07	0.2	
556	2, 7, 8, trans.	0.04	0.08	0.11	0.15	
558	10	0.02	0.04	0.03	0.15	
560	3, 5,	0.01	0.02	0.06	0.04	
570	2, 7, trans.	0.06	0.1	0.08	0.12	
572	9	0.02	0.04	0.02	0.09	
584	Original Oil	0.50	0.45	0.38	0.33	
598	2	0.02	0.12	0.15	0.19	
600	3	0.00	0.05	0.03	0.1	
612	2	0.02	0.04	0.05	0.09	
614	--	0.01	0.03	0.01	0.08	
616	3, 5,	0.01	0.02	0	0.05	
626	2	0.02	0.04	0.03	0.05	
640	Original Oil	0.10	0.1	0.06	0.06	

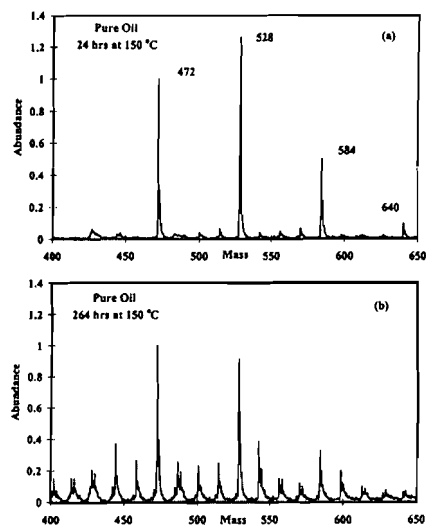


Fig. 1—Mass spectrum of pure oil aged at 150°C measured by LDMS.  
(a) 24 hrs  
(b) 264 hrs. The molecular weights of the tetraesters in the original oil are indicated near their mass peaks in (a).

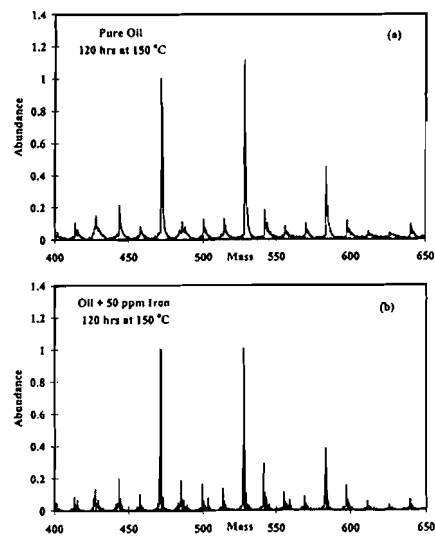


Fig. 2—Mass spectrum of oil aged at 150°C measured by LDMS.  
(a) pure oil, 24 hrs  
(b) oil containing 50 ppm of dissolved iron, 264 hrs

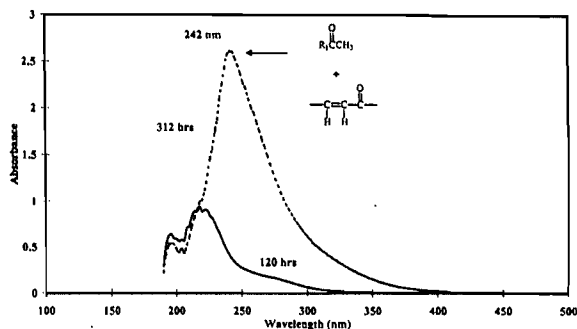
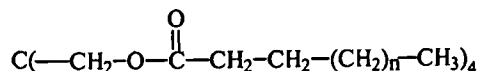


Fig. 3—UV absorption spectrum of oil aged at 150°C for 120 hrs, solid curve, and 312 hrs, dashed curve. Reference spectrum was unaged pure oil.

weight 528.73), 584 for the pentaerythritol tetraheptanoate (exact molecular weight 584.83), and 640 for the pentaerythritol tetraoctanoate (exact molecular weight 640.94). From the LDMS abundance peak heights shown in Fig. 1(a), the commercial pentaerythritol tetraester oil



was made up of a mixture of pentaerythritol tetrapentanoate ( $n=1$ ), pentaerythritol tetrahexanoate ( $n=2$ ), pentaerythritol tetraheptanoate ( $n=3$ ), and pentaerythritol tetraoctanoate ( $n=4$ ) in a 1:1.26:0.5:0.1 mole ratio. Figure 1(b) shows the mass spectrum of the pure oil sample aged for 264 hrs at 150°C. The mass spectra for pure oil, and oil containing 50 ppm of dissolved iron, aged 120 hrs at 150°C, are shown in Figs. 2(a) and 2(b), respectively.

The UV absorbance spectra of pure oil aged for 120, and 312, hrs at 150°C are shown in Fig. 3.

The relative viscosity, and UV maximum absorbance as a function of time during aging at 150°C are shown in Fig. 4 for pure oil, and oil containing 50 ppm of dissolved iron. The relative viscosity shown in Fig. 4(a) is the ratio of the sample viscosity at time  $t$  to the viscosity of the as-received oil (0.0361 Pa-sec at 20°C). The UV maximum absorbance between 200 and 300 nm, shown in Fig. 4(b), was smoothed (removing apparent noise fluctuations) in order to illustrate the observed trend of increase with time.

The proton NMR spectrum of the pentaerythritol tetraester oil is shown in Fig. 5, and the peak assignments with their chemical shift and integrated areas are listed in Table 2. The peak assignments were determined by comparison with the NMR spectrum of *n*-hexanoic acid. The NMR spectrum indicates the presence of some methyl side groups (branching) on the alkyl ester (doublet at 1.11 ppm). The ratio of the methyl side group protons to the pentaerythritol protons was unchanged by oxidation. The NMR integrated peak areas in Table 2 are consistent with the pentaerythritol tetraester oil being pentaerythritol hexanoate, or a mixture of the four components detected by LDMS. The distribution of molecular weights in the oil could not be determined from the NMR peak areas alone.

The FTIR absorbance spectrum of the pentaerythritol tetraester oil is shown in Fig. 6. The ester group peaks are at 1746.7 and

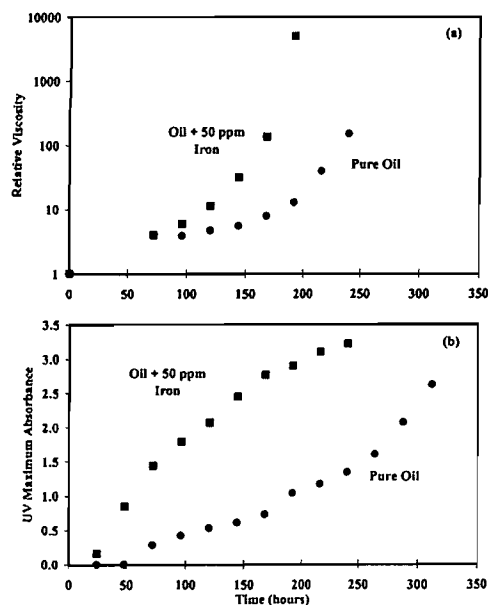


Fig. 4—Changes in the physical properties of the oil during aging at 150°C.

(a) relative viscosity

(b) UV absorbance maximum as a function of time. Filled circles are pure oil and filled squares are oil containing 50 ppm of dissolved iron.

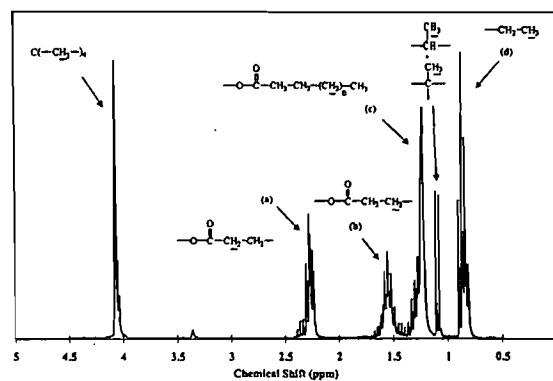


Fig. 5—Proton NMR spectrum of oil aged 24 hrs at 150°C.

1174.8  $1/\text{cm}$ , and the alkyl chain hydrocarbon group peaks are at 2952.5, 1453, and 1375.8  $1/\text{cm}$ . The peak assignments are shown in Fig. 6(a). A new hydrogen bonded hydroxyl peak at 3540  $1/\text{cm}$  is detected in the FTIR absorbance spectrum of the oil after aging, as illustrated in Fig. 6(b).

A developed and exposed TLC plate with the initial oil sample, oil aged for 144 hours, and for 168 hours, are shown by the three streaks in Fig. 7. The oil migrated vertically along the silica gel layer from the initial spot at time zero. The intensity of the streak is proportional to the areal density of oil on the plate at a given location. Each oil sample consists of at least two fractions having different polarity. The polarity increased with increasing oil oxidation. The initial oil consists of two fractions, the minor one being more polar than the major one. The aged oil consists of three fractions with different degrees of polarity. A significant fraction

PROTONS	CHEMICAL SHIFT (ppm)	RELATIVE PEAK AREA
$\alpha$ - <u>CH</u> -I	4.07	2
$-\text{OOCCH}_2\text{CH}_2\text{CH}_2\text{CH}_2$	2.27	1.8
$-\text{OOCCH}_2\text{CH}_2(\text{CH}_2)_2\text{CH}_2$	1.55	1.9
$-\text{OOCCH}_2\text{CH}_2\text{CH}_2\text{CH}_2$	1.23	4.1
$-\text{OOCCH}_2\text{CH}_2\text{CH}_2\text{CH}_2$	0.87	2.9
$-\text{OCH}_2-$ : $-\text{C}(\text{CH}_2)-$	1.11	0.6

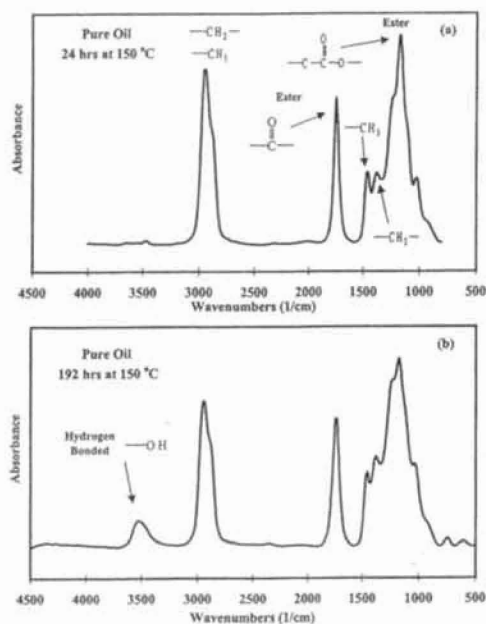


Fig. 6—FTIR spectrum of oil aged at 150°C.  
(a) 24 hrs  
(b) 192 hrs

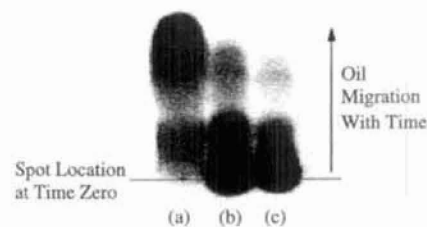


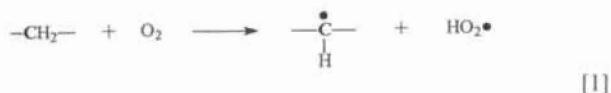
Fig. 7—Thin layer chromatography plate.  
(a) initial oil  
(b) oil aged 144 hours  
(c) oil aged 168 hours at 150°C

of the aged oil was so polar that it remained in its original location, as indicated by the dark circular regions in the lower part of Figs. 7(b) and 7(c).

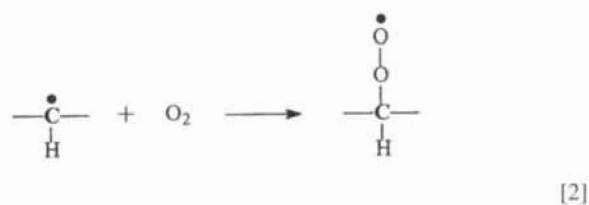
## DISCUSSION

### Oxidation Chemistry

The discussion focuses on the reaction pathways leading to the products observed in this study. The oxidation reaction sequence starts with formation of a carbon radical on the alkyl chain. The original carbon on which the radical was formed is indicated in bold face type:



The following description of the oxidation mechanism is based on Refs. (6)-(8). The carbon radical reacts with an oxygen molecule to form a peroxy radical:

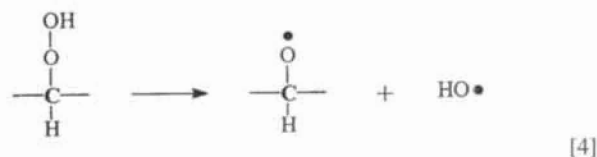


The peroxy radical then abstracts a proton from an alkyl chain:

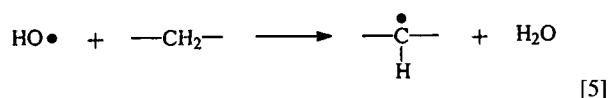


The alkyl chain from which the proton is abstracted may be the same one which already contains the peroxy radical, intrachain abstraction. Alternatively, the peroxy radical may abstract a proton from a different alkyl chain, interchain abstraction. The abstraction of a proton by the peroxy radical forms a hydroperoxide and a carbon radical.

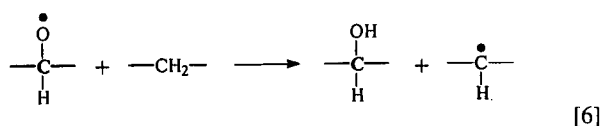
The sequence of reactions resulting from interchain proton abstractions is described first. The hydroperoxide decomposes into an alkoxy radical and a hydroxy radical:



The hydroxy radical abstracts a proton from an alkyl chain to produce a carbon radical and water:

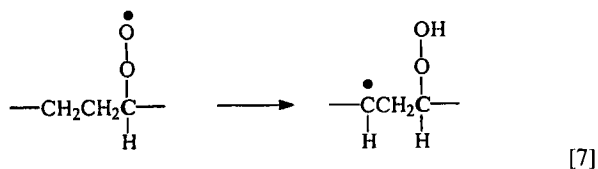


The alkoxy radical also abstracts a proton from an alkyl chain forming a carbon radical and a hydroxyl group in the alkyl chain on which the carbon radical initially formed:

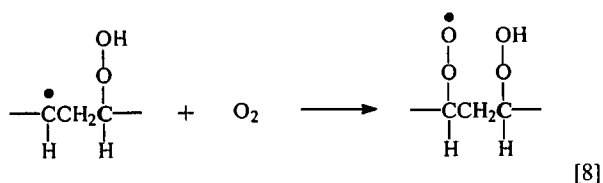


Within the interchain reaction pathway, one carbon radical gives rise to the formation of three new carbon radicals, chain propagation.

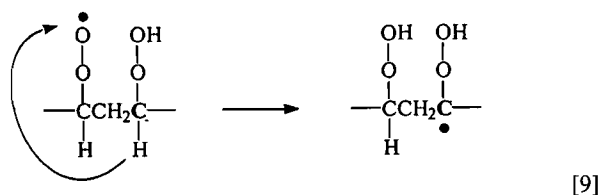
The peroxy radical formed in reaction Eq. [2] can also bring about intrachain proton abstraction, which forms a different set of products as shown in the following reaction sequence. The authors first consider ( $\alpha$ ,  $\gamma$ )-abstraction, which forms a  $\gamma$ -hydroperoxy carbon radical:



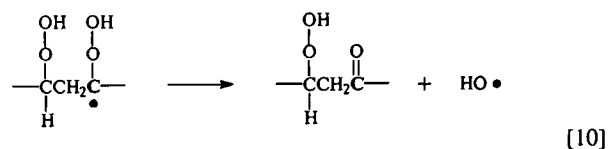
The  $\gamma$ -carbon radical reacts with oxygen to form a  $\gamma$ -hydroperoxy-peroxy radical:



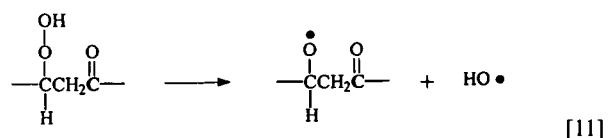
This peroxy radical abstracts the proton from the carbon carrying the hydroperoxide, forming an intermediate dihydroperoxide radical species:



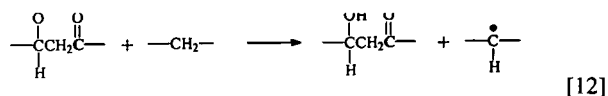
The hydroperoxide-carbon radical decomposes into a hydroperoxy ketone and a hydroxy radical:



The remaining hydroperoxy ketone decomposes into an alkoxy radical and a hydroxy radical:

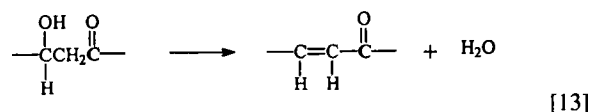


The alkoxy radical abstracts a proton from another alkyl chain, forming a  $\beta$ -hydroxy ketone and a carbon radical:



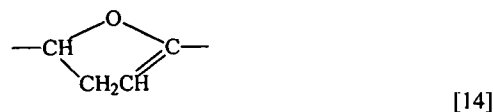
Instead of reaction Eq. [7], ( $\alpha$ ,  $\delta$ )-abstraction may occur. The same series of subsequent reactions, Eqs. [8] through [12], then leads to formation of  $\gamma$ -hydroxy ketones.

The  $\beta$ -hydroxy ketone dehydrates, leaving an unsaturated ketone on the alkyl chain:

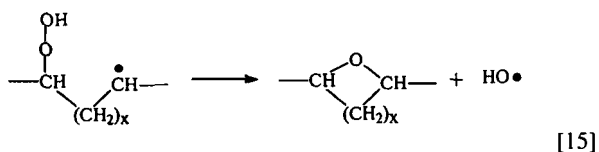


The unsaturated ketone produces the observed increase in the UV/visible absorbance spectrum with accelerated aging, as shown in Figs. 3 and 4(b), arising from  $n \rightarrow \pi^*$  transitions of conjugated ketones. These also may contribute to the brown coloration of the oil observed in the later stages of accelerated aging.

Two other types of oxygenated products are expected to arise from intrachain proton abstraction. 2,5 di-substituted dihydrofuran results from cyclization and dehydration of an ( $\alpha$ ,  $\delta$ )-hydroxyketone (6)

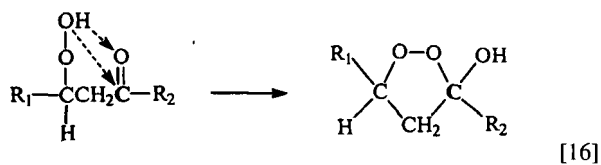


In the presence of lower oxygen concentrations, the ( $\alpha$ ,  $\gamma$ )- and ( $\alpha$ ,  $\delta$ )-monohydroperoxy carbon radicals, reaction Eq. [7], may undergo significant cyclization to form substituted oxetanes (6) with the loss of hydroxy radical:

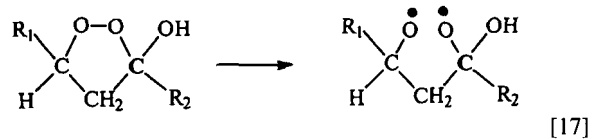


where  $x$  is 1 or 2.

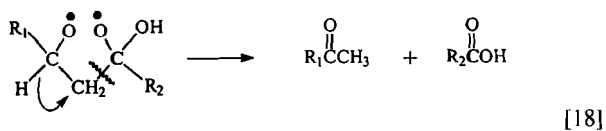
The sequence of intrachain proton abstraction reactions leading to chain cleavage and formation of new carboxylic acid and methyl ketones (7) is now described. A parallel reaction pathway to reaction Eq. [11], leading to the dioxolane intermediate, is given by reaction Eq. [16]:



The most likely hydroperoxy ketone, product of reaction Eq. [10], is formed starting with a radical on the carbon next to the methyl group on an alkyl chain,  $R_2 = \text{CH}_3$ .  $R_1$  is the rest of the tetraester molecule. The product on the right hand side of reaction Eq. [16] is a 3-hydroxy-3,5-alkyl-1,2-dioxolane. A 1,5 diradical intermediate is produced by homolysis of the peroxy bond (12):



The diradical decomposes through  $\beta$  scission with rearrangement by group migration. The only type of migration consistent with the distribution of oxidation products of pentaerythritol tetraheptanoate reported in Ref. (8) (Table 5) is proton migration with scission as shown below.



In reaction Eq. [18], the  $R_1$  and  $R_2$  groups are the remaining portion of the alkyl chain on either side of the diradical. Alkyl chain cleavage through intramolecular proton abstraction leaves either a methyl ketone or a carboxylic acid end attached to the original pentaerythritol tetraester molecule. Note that the most likely hydroperoxy ketone, where  $R_2 = \text{CH}_3$ , leads to the formation of a methyl ketone end group and acetic acid.

Thus, one result of the intrachain proton abstraction by a peroxy radical is cleavage of an alkyl ester chain on the pentaerythritol tetraester molecule. Notice that this cleavage process involves

proton abstraction from carbons at each end of a 3-carbon segment of the alkyl ester chain. The free energy change for abstraction of a proton from the methyl carbon or from the methylene carbon next to the carboxyl group of the alkyl ester is larger than that for abstraction of a proton from the "internal" methylene carbons. Therefore, the rate of chain cleavage through intrachain proton abstraction is expected to decrease with decreasing alkyl chain length in the series order (octanoate > heptanoate > hexanoate > pentanoate). In particular, the pentanoate should be especially unreactive since it does not contain 3 "internal"  $\text{CH}_2$  groups. Nakanishi et al. (13) studied the effect of alkyl ester chain length on the oxidation stability of pentaerythritol tetraesters. They found that alkyl ester chains pentanoate and shorter were less reactive than hexanoate and lasted longer in corrosion oxidation stability tests at 230°C.

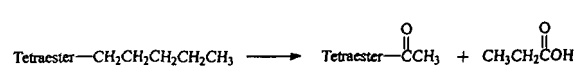
### LDMS Analysis

The oxidation products give rise to new mass peaks observed with LDMS, Figs. 1(b), and 2. The mass peaks, and their relative abundance, are listed in Table 1. The origin of the mass peaks detected in the aged oil samples is described as follows.

1. Mass gain in multiples of 12, unsaturated ketone, reaction Eq. [13] or 2,5 substituted tetrahydrofuran, reaction Eq. [14].
2. Mass gain in multiples of 14, substituted oxetanes, reaction Eq. [15].
3. Mass gain in multiples of 16, hydroxyl, reaction Eq. [6].
4. Mass gain in multiples of 30,  $\beta$  hydroxy ketone, reaction Eq. [12].
5. Mass gain in multiples of 32, hydroperoxide, reaction Eq. [3].
6. Mass gain in multiples of 46,  $\beta$  hydroperoxy ketone, reaction Eq. [10] or 3-hydroxy-3,5-alkyl-1,2-dioxolane, reaction Eq. [16].
7. Mass loss in multiples of 14, methyl ketone on the alkyl ester attached to the pentaerythritol formed with the loss of acetic acid (reaction Eq. [16] with  $R_2 = \text{CH}_3$  -).



8. Mass loss in multiples of 28, methyl ketone on the alkyl ester attached to the pentaerythritol formed with the loss of propanoic acid (reaction Eq. [16] with  $R_2 = \text{CH}_3\text{CH}_2$  -).

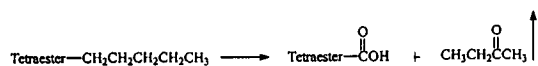


9. Mass loss in multiples of 12, carboxylic acid on the alkyl ester attached to the pentaerythritol formed with the loss of acetone (reaction Eq. [16] with  $R_1 = \text{CH}_3$  -).





10. Mass loss in multiples of 26, carboxylic acid on the alkyl ester attached to the pentaerythritol formed with the loss of 2-butanone (reaction Eq. [16] with  $R_1 = \text{CH}_3\text{CH}_2-$ ).



New mass peaks may also arise during the accelerated aging of the oil by rearrangement of the tetraester monomers through interchange of the ester chains, or transesterification. The pentaerythritol tetrapentanoate mass can only be increased by transesterification as  $m \times 14 + p \times 28$ , with  $m, p = 0, 1, 2, 3$  or 4, and  $m + p \leq 4$ . The pentaerythritol tetrahexanoate mass can be increased or decreased as  $(m + p) \times 14$  with  $m = 0, 1, 2, 3$  or 4,  $p = 0, -1, -2, -3$  or 4, and  $m + p \leq 4$ . **NEGLECTING THE SMALL AMOUNT OF OCTANOATE**, the pentaerythritol tetraheptanoate mass can only be decreased as  $m \times 14 + p \times 28$  with  $m, p = 0, -1, -2, -3$  or 4, and  $m + p \leq 4$ .

The assignment of the mass peaks to the oxidation products, described 1 through 10 above, are indicated in the column next to the molecular weights in Table 1. The new mass peaks which could arise from ester interchange, or transesterification, are indicated by (trans.) in Table 1. An observed mass often may result from more than one type of product. Further complexity, which is not taken into account by this analysis, arises from combinations of two or more different types of oxidation product on the same tetraester molecule.

The mass peaks found in the oxidized oil were compared with those expected from oxidation reactions Eqs. [1] through [18]. The mass peaks from products 1 through 10 were calculated for multiples of 1, 2, 3 and 4. The mass peaks calculated from each source were superimposed on the measured mass spectra from the aged oil shown in Figs. 1(b) and 2. Products consistent with the observed mass peaks were identified. Mass peaks below the original pentaerythritol tetrapentanoate peak at 472 must arise from chain cleavage. The peaks at 416, 430, 444 and 458 are consistent with the formation of cleavage products with methyl ketone end groups, products 7 and 8. The unassigned mass peaks at 402, 414 and 428 may arise from oxidation products formed on a tetraester with cleaved chains.

Intermediate mass peaks, between the original pentaerythritol tetrapentanoate, hexanoate, and heptanoate, arise from oxidation products in addition to those formed by chain cleavage. Transesterification can account for some of the intermediate mass peaks at 486, 500, 514, 542, 556 and 570. Other intermediate mass peaks are consistent with the presence of cleavage products having one acid end group formed on pentaerythritol tetrahexanoate, 516, or on pentaerythritol tetraheptanoate, 558 and 572, products 9 and 10. Acid groups formed on the pentaerythritol tetrapentanoate were not detected.

Mass peaks above 584 arise from increased molecular weight of oxidation products. The presence of 1, 2, 3 and 4 substituted oxetanes formed on a pentaerythritol tetraheptanoate is consistent with the mass peaks at 598, 612, 626, and 640, respectively, products 2. Single hydroxyl groups formed on pentaerythritol tetrapen-

tanoate, hexanoate, and heptanoate give rise to the mass peaks at 488, 544, and 600, respectively, products 3. Mass peaks at 504, 560 and 616 are consistent with either two hydroxyl groups or a single hydroperoxide group, 5, on each of the three tetraesters.

After 120 hours of accelerated aging at 150°C, the oil containing 50 ppm of dissolved iron seemed to include more tetraesters with single oxetane groups than the pure oil after the same treatment, mass peaks at 486, 542, and 598, products 2. Increased aging time from 120 to 264 hours for the pure oil increased the amount of tetraesters with methyl ketone end groups, products 7 and 8 and cleavage acids 9 and 10. The amount of hydroxyl groups 3 greatly increased between 120 and 264 hours.

Certain peaks were absent from the mass spectrum. Mass peaks due to unsaturated ketone or 2,5 substituted tetrahydrofuran 1 were not found. There were no mass peaks that could be attributed to  $\beta$ -hydroxy ketone 4,  $\beta$ -hydroperoxy ketone, or 3-hydroxy-3,5-alkyl-1,2 dioxolane 6.

The height of the mass peaks shown in Table 1 were examined to look for differences in the oxidation product distribution. Increasing the aging time of the pure oil from 120 to 264 hours increased the concentrations of all oxidation products except those having four oxetanes formed on a pentaerythritol tetraheptanoate, which decreased. The largest increases were in products with multiple methyl ketone end groups, one hydroxyl group, two hydroxyl groups or one hydroperoxide group, oxetanes, and acid end groups on pentaerythritol tetrahexanoate and heptanoate.

The effect of 50 ppm of iron dissolved in the oil was compared to the product distribution of the pure oil after aging for 120 hours. Fewer methyl ketones and acid end groups were detected with the iron present. There were also fewer tetraesters with single hydroxyl groups. In the presence of the dissolved iron, there were more of all three tetraesters with one or two oxetanes. The largest increase found in the oil containing dissolved iron was in two hydroxyl groups, or one hydroperoxy group, formed on pentaerythritol tetrapentanoate and hexanoate.

The product distribution in the pure oil aged for 264 hours was compared with the oil containing 50 ppm of iron aged for 120 hours. All the products were less in the oil with iron except for tetraesters with two hydroxyl groups, or one hydroperoxy group, formed on pentaerythritol tetrapentanoate and hexanoate, of which there was considerably more present in the oil containing iron, even though it was aged for less than half the time. It seems that the dissolved iron increases the rate of hydroxyl (or hydroperoxy) and oxetane group formation and decreases the rate of chain cleavage.

Overall, the abundance of the pentaerythritol tetrahexanoate and heptanoate decreased relative to that of the pentanoate, and the heptanoate decreased more than the hexanoate. This is attributed to the increasing number and reactivity of protons available for intrachain proton abstraction, leading to chain cleavage, with increasing chain length. This could not be from oil evaporation, because evaporation would have removed the lower molecular weight pentaerythritol tetrapentanoate faster than the higher molecular weight pentaerythritol tetrahexanoate.

The mass spectrum was examined for the presence of dimers formed by transesterification between pentaerythritol tetraheptanoate with one acid end group by displacement of a heptanoic

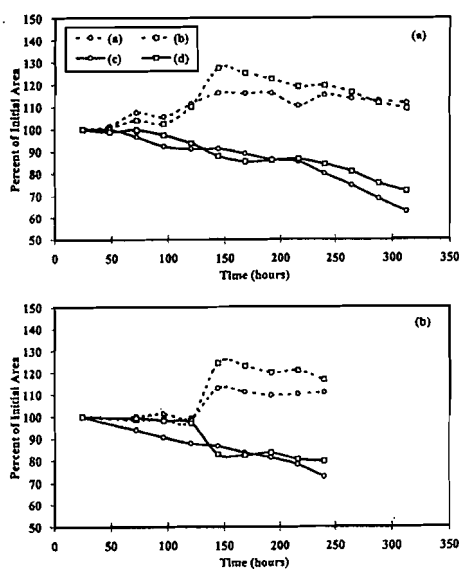


Fig. 8—Proton NMR peak areas plotted as a percent of the initial peak area as a function of time at 150°C.

(a) pure oil

(b) oil containing 50 ppm of dissolved iron. Curves (a), (b), (c), and (d) correspond to the letters on the peaks in Fig. 5. The letters denote: (a)  $\alpha$ -CH<sub>2</sub>, (b)  $\beta$ -CH<sub>2</sub>, (c) internal-CH<sub>2</sub>, and (d) end-CH<sub>3</sub>.

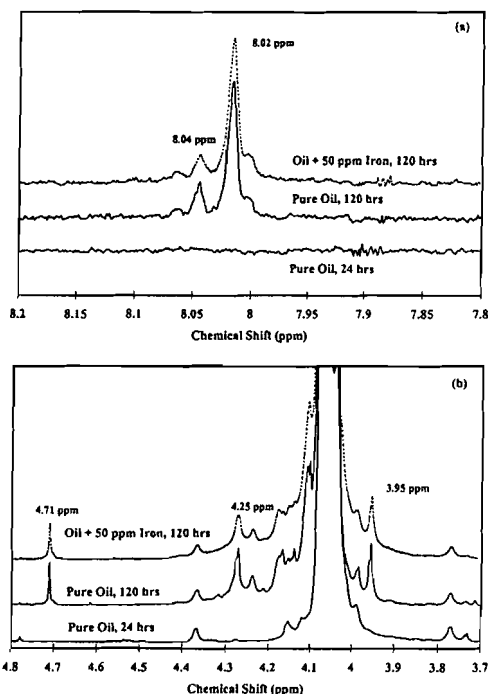


Fig. 9—Proton NMR spectra expanded to show the region near (a) and (b).

(a) 8 ppm  
(b) 4 ppm

acid chain from another pentaerythritol tetraheptanoate. The heptanoate is the most likely tetraester to be found with an acid end group. (The octanoate is actually the most likely to acquire an acid end group, but there is only a small amount of the octanoate pres-

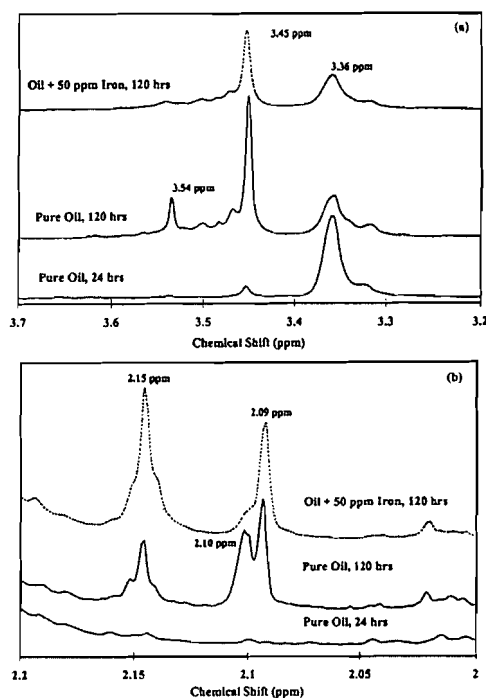


Fig. 10—Proton NMR spectra expanded to show the region near (a) and (b).

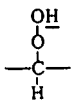
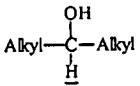
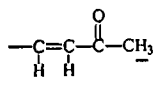
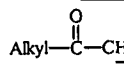
(a) 3.5 ppm  
(b) 2.1 ppm

ent in the initial oil.) The diacid ester linkage was either propanedioic or butanedioic acid. These chemical dimers were not found in the mass spectrum. The masses in this region are of Van Der Waals dimers, which are formed among the tetraesters and their oxidation products in the vapor phase during jet cooling after laser desorption. The Van Der Waals dimers differ from chemical dimers with the same number of carbons by 2 mass units. The formation of oligomers (2), (9) may occur only at higher temperatures or in the presence of solid metal catalyst.

### NMR Analysis

The changes in the proton NMR spectrum integrated peak areas with time during the accelerated aging test show the loss of methyl and methylene protons, and the formation of protons adjacent to carboxylate ester groups. The peaks from the methyl and methylene protons are indicated in Fig. 5 as (c) and (d), respectively. The peaks from the protons  $\alpha$  and  $\beta$  to the carboxylate ester groups are indicated in Fig. 5 as (a) and (b), respectively. Peak areas were integrated from NMR spectra measured on samples drawn from the oil as a function of time during the accelerated aging test at 150°C. To highlight the changes in the sample composition, the peak areas are shown plotted as per cent of the initial peak area in Fig. 8. (Percent of initial area = 100 x area at time  $t$  / initial peak area.) Figure 8(a) shows the results from aging of pure oil, and Fig. 8(b) shows the result from aging oil containing 50 ppm of dissolved iron. In both cases, the changes in the NMR peaks reflect the results of intrachain proton abstraction which leads to loss of methylene and methyl protons through evaporation of low molecular weight cleavage products. This gives rise to

TABLE 3—PEAK ASSIGNMENTS FOR SOME OF THE SMALL NMR PEAKS OBSERVED DURING THE ACCELERATED AGING TEST AT 150°C. PROTONS RESPONDING AT THE INDICATED CHEMICAL SHIFT ARE INDICATED BY AN UNDERScore. PEAKS FOR WHICH ASSIGNMENT WAS NOT MADE ARE INDICATED BY A DASH IN THE PROTONS COLUMN.

PROTONS	CHEMICAL SHIFT (ppm)
	8.02
—	4.71
	3.45, 3.54
—	3.36
	2.15
	2.09

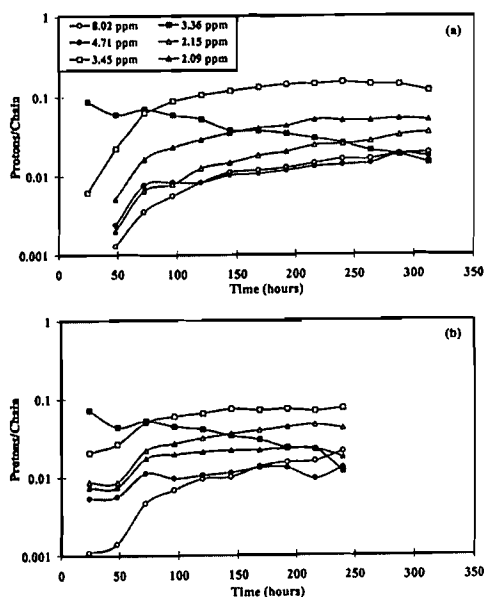


Fig. 11—Protons per chain for the small NMR peaks associated with oxidation products listed in Table 3 as a function of time at 150°C.

(a) pure oil  
(b) oil containing 50 ppm of dissolved iron

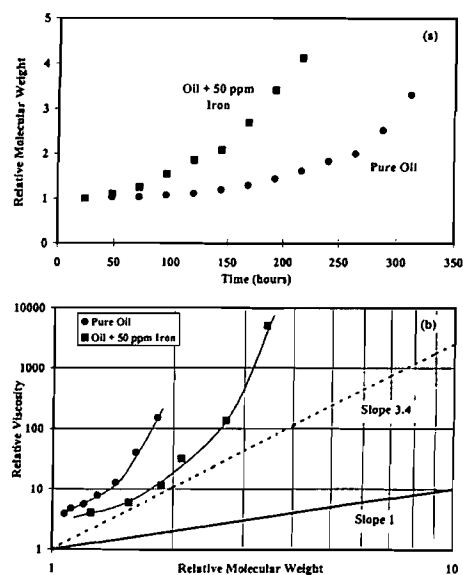


Fig. 12—The relationship between molecular weight and viscosity during aging at 150°C.  
(a) relative molecular weight from GPC as a function of time  
(b) relative viscosity as a function of relative molecular weight. The viscosity increased much faster than could be expected from the known dependence on molecular weight.

TABLE 4—THE GLASS TRANSITION TEMPERATURE  $T_g$  OF THE PENTAERYTHRITOL TETRAESTER OIL BEFORE ACCELERATED AGING AND AFTER AGING FOR DIFFERENT AMOUNTS OF TIME AT 150°C.

SAMPLE	TIME AT 150°C (hrs)	$T_g$ (°C)
Pure Oil	0	-88.1
	192	-69.4
	240	-54
Oil + 50 ppm Iron	192	-53.4

the more or less steady decrease of groups (c) and (d), Fig. 8. The peaks (a) and (b) are assigned to the protons  $\alpha$  and  $\beta$  to the carboxylic acid group in the initial tetraester. Peaks (a) and (b) with the same chemical shift also can be assigned to the protons  $\alpha$  and  $\beta$  to the carbonyl group of methyl ketone end groups formed by chain cleavage, reaction Eq. [18], products 7 and 8. The increase in peaks (a) and (b) in Fig. 8 is due to the formation of methyl ketone and carboxyl end groups on alkyl chains. There is an apparent induction period because these groups do not form until there is a significant buildup of  $\beta$ -hydroperoxy ketone, reaction Eq. [10]. The gradual decrease with time of peaks (a) and (b) is due to loss of the lower molecular weight oxidation products through evaporation, the gradual decrease of peak (c) and (d) is due to oxidation reaction of these "internal" protons, and the gradual decrease of peak (d) is due to loss of methyl end groups through formation of methyl ketone end groups.

Small peaks associated with oxidation products were also observed in the NMR spectrum. Expanded regions of the NMR spectra illustrating these small peaks are shown in Figs. 9 and 10, for the oil before aging and after aging for 120 hours at 150°C with and without 50 ppm of dissolved iron. The peak assignments for several of the small NMR peaks are listed in Table 3. Peak assign-

ments were made by comparison with spectra of known compounds with similar substituents in the Aldrich spectra library (14) and/or by calculation using a table of substituent effects on chemical shift (15). The NMR spectra were also measured following addition of D<sub>2</sub>O to exchange with hydroxyl protons. There was no difference in the NMR spectra following deuterium exchange of hydroxyl protons.

The NMR peaks in Table 3 were integrated to follow the changes as a function of accelerated aging time at 150°C. The protons at 3.45 and 3.54 were separated from other peaks but close to one another, so they were integrated together. The peak areas were converted to the number of protons per chain. The protons/chain = 2x(integrated area of a small peak/integrated area of protons at 4.07 ppm). The protons/chain at the chemical shifts listed in Table 3 are shown plotted as a function of time in Fig. 11. The only peak that decreased with time was the one at 3.36 ppm. This proton starts out at about 0.1/chain.

The protons/chain as a function of time for each type of proton was examined to study any effects of dissolved iron on their relative concentration and formation rates. The hydroperoxide concentration was unchanged by the presence of dissolved iron in the oil. The concentration of protons at 4.71 ppm was initially higher in the presence of iron and reached a steady level which remained nearly constant at the same level with and without dissolved iron after 72 hours. The concentration of protons at 3.36 ppm was slightly lower with dissolved iron and decreased at the same rate both with and without dissolved iron. The concentration of protons at 3.45 ppm was initially higher with dissolved iron and then became less than without iron and both reached nearly steady state after about 100 hours. This is attributed to the formation of multiple hydroxyl groups on the same chain in the presence of the iron which shifts the original proton away from 3.45 ppm. The concentration of protons at 2.15 ppm was significantly higher in the presence of iron and increased at nearly the same rate with and without iron. The protons at 2.09 ppm reached a steady value after about 72 hours in the oil containing iron, while in the pure oil they exceeded their concentration in the presence of iron and continued gradually increasing with time. This is probably due to the conversion of hydroperoxy ketones to unsaturated methyl ketones at a higher rate in the presence of dissolved iron.

The activation energy for the overall reaction was calculated from an Arrhenius plot made using the rate of increase in the maximum UV/visible absorbance at 130°, 140°, 150°, 160° and 170°C. The activation energy for the pure oil was 120 kJ/mole. This is in fair agreement with the activation energy of 125 kJ/mole for pentaerythritol tetraheptanoate reported by Hamilton et al. (8). The reaction rate for oil containing 50 or 100 ppm of dissolved iron was much higher than that of the pure oil, and changed little over this range of temperature, so that an activation energy could not be determined.

## VISCOSITY AND HYDROGEN BONDING

Chemical degradation of ester oil has been reported to produce higher molecular weight, oligomeric, products based on GPC measurements (2), (9). The relative molecular weight calculated from the GPC elution curve as a function of time during aging at

150°C is shown in Fig. 12(a) for pure oil and oil containing 50 ppm iron. The relative molecular weight is the ratio of the aged sample molecular weight from GPC to the molecular weight after aging for 24 hrs at 150°C. (There was no change in molecular weight after aging for 24 hrs at 150°C.) The increase in viscosity during accelerated aging was compared with the increase in molecular weight from GPC. The relative viscosity is shown plotted as a function of the relative molecular weight in Fig. 12(b). Below the entanglement molecular weight, the viscosity of a polymer melt or solution is proportional to the polymer molecular weight, while above the entanglement molecular weight the viscosity is proportional to the 3.4 power of the molecular weight (16). The molecular weight of the aged oil is well below the entanglement molecular weight, so the viscosity was expected to be proportional to the molecular weight. The measured viscosity, shown by the symbols in Fig. 12(b), increased much more rapidly than could be attributed to the apparent increase in molecular weight from GPC.

The apparent increase in molecular weight is determined from the GPC elution curve and the calibration for the column using species of known molecular weight. The retention time is determined by the hydrodynamic volume of diffusing species in the eluent. The hydrodynamic volume is generally assumed to be a function of the molecular weight. However; in the case of molecular association, the retention time is determined by the hydrodynamic volume of the associated species (17).

The possibility of association between hydroxyl or acid functionalized hydrocarbons in our GPC column was investigated. The elution curves were measured for linear C<sub>26</sub>H<sub>54</sub>, its alcohol C<sub>26</sub>H<sub>53</sub>OH, and the carboxylic acid C<sub>26</sub>H<sub>53</sub>OOH. Using the standard procedure for calculating molecular weight from the elution curve, the alcohol and the acid appeared to have twice the molecular weight of the linear C<sub>26</sub>H<sub>54</sub>. The acid and alcohol were associated into dimers and, thus, had twice the hydrodynamic volume of a monomer, which caused it to show up as an apparent increase in molecular weight. A similar association between oxidized pentaerythritol tetraesters containing primarily hydroxyl and some acid functional groups must also take place during the GPC measurements. Therefore, the apparent molecular weight increase of the oil with aging in Fig. 12 is actually an increase in the degree of association between oxidized tetraesters. As described in the LDMS Analysis section, chemical dimers (and low molecular weight polymers or oligomers) were absent from the LDMS spectrum.

The increase in viscosity is accounted for by the presence of intermolecular hydrogen bonding between the hydroxyl groups formed on alkyl chains. Hydrogen bonding increases the energy barrier to cooperative rearrangement necessary for flow (18), (19). The contribution of hydrogen bonding to the viscosity increases with time during the accelerated aging test due to the formation of more hydroxyl groups with time.

The increase in the intermolecular interaction energy through hydrogen bonding between hydroxyl groups formed as a result of oxidation shows up as an increase in the glass transition temperature T<sub>g</sub> (19). The T<sub>g</sub> for oil samples with and without dissolved iron aged at 150°C is listed in Table 4. The T<sub>g</sub> of the pure oil increased with time. The T<sub>g</sub> of the oil containing 50 ppm of iron

after 192 hrs at 150°C was close to the  $T_g$  of the pure oil after 240 hrs at 150°C. This indicates that the hydroxyl content of these two samples was nearly the same in each case, because they both exhibited the same increase in  $T_g$ . The change in heat capacity at the glass transition temperature was  $\approx 0.5$  J/g for all of the samples listed in Table 4.

Thin layer chromatography graphically illustrates the increase in polarity resulting from hydroxyl group formation, Fig. 7. The streak on the left shows how far the initial oil traveled along the plate in a given period of time, Fig. 7(a). The streaks of oil aged for 144 hours, Fig. 7(b), and for 168 hours, Fig. 7(c), traveled progressively less than the initial oil in the same amount of time. The hydrogen bonding between the functional groups on the oil and the silica gel lowers the oil mobility.

The presence of intermolecular hydrogen bonding is consistent with the appearance of a broad hydroxyl peak near 3500  $1/\text{cm}$  in the FTIR absorbance spectrum of the oils after aging at 150°C, Fig. 6.

Observed changes in solubility with aging are consistent with an increase in the polarity of the oil. The pentaerythritol tetraester oil was initially soluble in both heptane and cyclohexane and became insoluble in either of these two solvents after oxidation.

Therefore, the increase in viscosity with accelerated aging of the pentaerythritol tetraester oil is due to intermolecular hydrogen bonding between hydroxyl groups formed on the alkyl chains.

## SUMMARY AND CONCLUSIONS

The oxidation chemistry was studied during accelerated aging of a commercial pentaerythritol tetraester oil lubricant base stock. The oil was found to consist of a mixture of pentaerythritol tetrapentanoate, pentaerythritol tetrahexanoate, pentaerythritol tetraheptanoate, and pentaerythritol tetraoctanoate. The pure oil, and oil containing 50 or 100 ppm of dissolved iron, was aged at 130°, 140°, 150°, 160° or 170°C in air. Samples were taken each 24 hrs and analyzed using UV/visible spectroscopy, laser desorption mass spectrometry, infrared spectroscopy, nuclear magnetic resonance spectroscopy, gel permeation chromatography, thin layer chromatography, and viscometry.

The results of the analysis were interpreted within the framework of a pentaerythritol tetraester oxidation mechanism (6)-(8). Oxidation leads to conjugated ketones which are observed as increased UV absorbance. The molecular weights detected in the mass spectrum are consistent with the formation of hydroxyl groups, oxetane, and alkyl chain cleavage products. Changes in the proton nuclear magnetic resonance peak areas show the loss of methyl and methylene protons, and the formation of peroxides, hydroxyl groups, and saturated and unsaturated methyl ketone end groups.

The concentration of hydroperoxide was unchanged by the presence of dissolved iron, indicating that the rate of hydroperoxide formation and decomposition is independent of iron catalysis. Dissolved iron increased the rate of hydroxyl and oxetane formation, and decreased the rate of chain cleavage.

The increase in viscosity with aging was due to increasing intermolecular hydrogen bonding rather than an increase in molecular weight.

## ACKNOWLEDGEMENT

The authors are grateful to C. Wade, J. Kaufman, J. Lyerla, and C. Ortiz for their encouragement and support. Thanks are also due to M. Bower and M. Sherwood for assistance with the NMR measurements and analysis, C. Hawker for assistance with the GPC measurements, and S. Karandikar for TLC measurements. The authors thank R. Siemens for the glass transition temperature measurements. This work was done as a joint effort between the IBM Research Division, Almaden Research Center, and the IBM Storage Systems Division. One of us, DAH, was funded in part by NSF Grant 9300131 and Dreyfus Foundation Grant 5G94-120 to San Jose State University.

## REFERENCES

- (1) Klaus, E. E., Tewksbury, E. J. and Fietelson, S. S., "Thermal Characteristics of Some Organic Esters," *Trib. Trans.*, **13**, 1, pp 11-20, (1970).
- (2) Ali, A., Lockwood, F., Klaus, E. E., Duda, J. L. and Tewksbury, E. J., "The Chemical Degradation of Ester Lubricants," *Trib. Trans.*, **22**, 3, pp 267-276, (1979).
- (3) Cvitkovic, B., Klaus, E. E. and Lockwood, F., "A Thin Film Test for Measurement of the Oxidation and Evaporation of Ester-Type Lubricants," *Trib. Trans.*, **22**, 4, pp 395-401, (1979).
- (4) Lockwood, F. and Klaus, E. E., "Ester Oxidation- The Effects of an Iron Surface," *Trib. Trans.*, **25**, 2, pp 236-244, (1982).
- (5) Clark, D. B., Klaus, E. E. and Hsu, S. M., "The Role of Iron and Copper in the Oxidation Degradation of Lubricating Oils," *Lubr. Eng.*, **41**, 5, pp 280-287, (1985).
- (6) Jensen, R. K., Korcek, S., Mahoney, L. R. and Zinbo, M., "Liquid-Phase Autoxidation of Organic Compounds at Elevated Temperatures Part I—Stirred Flow Reactor Technique and Analysis of Primary Products from n-Hexadecane Autoxidation at 120-180°C," *Jour. Am. Chem. Soc.*, **101**, 25, pp 7574-7584, (1979).
- (7) Jensen, R. K., Korcek, S., Mahoney, L. R., and Zinbo, M. "Liquid Phase Autoxidation of Organic Compounds at Elevated Temperatures Part 2— Kinetics and Mechanisms of the Formation of Cleavage Products in n-Hexadecane Autoxidation," *Jour. Am. Chem. Soc.*, **103**, 7, pp 1742-1749, (1981).
- (8) Hamilton, E. J., Jr., Korcek, S., Mahoney, L. R. and Zinbo, M., "Kinetics and Mechanism of the Autoxidation of Pentaerythrityl Tetraheptanoate at 180-220°C," *Int'l. Jour. Chem. Kin.*, **XII**, pp 577-603, (1980).
- (9) Fuchs, H.-J. and Zeman, A., "Polymer Formation During Thermal-Oxidative Ageing of Aviation Turbine Oils," *Jour. Synth. Lubr.*, **10**, pp 3-22, (1993).
- (10) Nir, E., Hunziker, H.E., and de Vries, M.S., "Fragment-Free Mass Spectrometric Analysis with Jet Cooling/VUV Photoionization," *Anal. Chem.*, **71**, pp 1674-1678, (1999).
- (11) Sosulina, L. N., Skryabina, T. G., Volobuev, N. K., Kotova, G. G. and Ostrovskaya, T. K., "Micromethods for the Investigation of Lubricating Grease Composition," *Chemistry and Technology of Fuels and Oils*, **16**, 9-10, pp 685-688, (1980).
- (12) Baumstark, A. L. and Vasquez, P. C., "Thermolysis of Pentasubstituted 3-Hydroxy-1,2-dioxolanes," *Jour. Heterocyclic Chem.*, **29**, pp 1781-1783, (1992).
- (13) Nakanishi, H., Onodera, K., Inoue, K., Yamada, Y. and Hirata, M., "Oxidation Stability of Synthetic Lubricants," *Lubr. Eng.*, **53**, 5, pp 29-37, (1997).
- (14) Pouchert, C. J. and Campbell, J. R., *Aldrich Library of NMR Spectra*, Aldrich Chemical Co., Milwaukee, WI, (1974).
- (15) Silverstein, R. M., Bassler, G. C. and Morrill, T. C., *Spectrometric Identification of Organic Compounds*, 3rd ed., John Wiley & Sons, Inc., New York, NY, (1974).
- (16) Berry, G. C. and Fox, T. G., "The Viscosity of Polymers and Their Concentrated Solutions," *Adv. Polymer Sci.*, **5**, pp 261-357, (1968).
- (17) Stevens, F. J., "Analysis of Protein-Protein Interaction by Simulation Size-Exclusion Chromatography: Application to Antibody-Antigen Association," *Biochemistry*, **25**, pp 981-993, (1986).
- (18) Kim, S.-J. and Karis, T. E., "Glass Formation from Low Molecular Weight Organic Melts," *Jour. Mater. Res.*, **10**, 8, pp 2128-2136, (1995).
- (19) Karis, T. E., Kim, S.-J., Gendler, P. L. and Cheng, Y. Y., "Organic Monomeric Glass Formation by Substituted Ethylenediamine," *Jour. Non-Cryst. Sol.*, **191**, pp 293-303, (1995).